Received: 26 July 2021 | Revised: 12 December 2021 | Accepted: 21 December 2021

DOI: 10.1111/geb.13454

Global Ecology and Biogeography | A Journal of Macroecology | WILEY

RESEARCH ARTICLE

The global contribution of roots to total soil respiration

Jinshi Jian[1,2] | Max Frissell[2,3] | Dalei Hao[4] | Xiaolu Tang[5,6] | Erin Berryman[7] | Ben Bond-Lamberty[2]

[1]State Key Laboratory of Soil Erosion and Dryland Farming on the Loess Plateau, Northwest A&F University, Yangling, China

[2]Pacific Northwest National Laboratory, Joint Global Change Research Institute at the University of Maryland–College Park, College Park, Maryland, USA

[3]Seattle University, Seattle, Washington, USA

[4]Atmospheric Sciences and Global Change Division, Pacific Northwest National Laboratory, Richland, Washington, USA

[5]College of Ecology and Environment, Chengdu University of Technology, Chengdu, China

[6]State Environmental Protection Key Laboratory of Synergetic Control and Joint Remediation for Soil & Water Pollution, Chengdu University of Technology, Chengdu, China

[7]U.S. Forest Service, Rocky Mountain Research Station, Forest Inventory & Analysis (FIA), Fort Collins, Colorado, USA

Correspondence
Jinshi Jian, State Key Laboratory of Soil Erosion and Dryland Farming on the Loess Plateau, Northwest A&F University, Yangling 712100, China.
Email: jinshi@vt.edu

Funding information
the US Department of Energy, Office of Science, Biological and Environmental Research as part of the Terrestrial Ecosystem Sciences Program, Grant/Award Number: DE-AC05-76RL01830; The second Tibetan Plateau Scientific Expedition and Research Program (STEP), Grant/Award Number: 2019QZKK0603

Editor: Sean Michaletz

Abstract

Aim: Soil respiration (R_S) is one of the largest fluxes in the global carbon cycle. It is composed of respiration by roots and heterotrophic organisms, with each component having distinctive drivers and sensitivities and, consequently, varying feedback potential to climate change. Global drivers of the total flux of R_S are widely studied and generally accepted, but our understanding of the factors governing its component fluxes lags far behind.

Location: Global.

Time period: 1962–2015.

Major taxa studied: Plant roots and soil microbes.

Methods: Combining a newly updated global database of R_S partitioning measurements with biotic and abiotic variables, we examined the world-wide distribution of the proportion of the annual root respiration (R_{root}) contribution to R_S (R_{root}:R_S). We investigated how R_{root}:R_S varies by ecosystem type, measurement method and climate. We used a random forest model to predict the relationship between field measurements of R_{root}:R_S (n = 880) and 14 biotic and abiotic factors, including climate, nitrogen deposition, soil, mycorrhiza, biomass and satellite-derived greenness. Finally, we present a global map of predicted R_{root}:R_S at 0.5° resolution.

Results: Consistent with previous studies, we found no clear trends of mean R_{root}:R_S across ecosystem types and measurement methods. The area-weighted overall mean of predicted R_{root}:R_S was .42 (SD ± .18; i.e., 42% of total global R_S was generated by plant roots). Predicted R_{root}:R_S and related environmental factors did exhibit clear spatial patterns between climatic regions, with higher R_{root}:R_S in dry and cold regions and lower R_{root}:R_S in temperate and tropical regions.

Main conclusions: Given that R_{root}:R_S is linked to plant carbon use efficiency (CUE, the ratio of net primary production to gross primary production), but generated from measurements completely independent of plant CUE, it might provide crucial insights into ecosystem- to global-scale carbon cycling. This study thus provides a framework to explore global carbon allocation under global climate change.

KEYWORDS
carbon cycling, carbon use efficiency, modelling, random forest, root respiration, soil respiration

1 | INTRODUCTION

Plant root respiration (R_{root}, from all roots) is an important carbon flux in terrestrial ecosystems, thought to release 40–50 Pg C/year to the atmosphere, approximately four times the amount of carbon released by fossil fuel combustion (Bond-Lamberty et al., 2004a; Hanson et al., 2000; Tang et al., 2019). The amount of R_{root} is thought to be determined by the root biomass, root nitrogen concentration, specific root length, mycorrhiza, root exudation, ecosystem production and allocation patterns of plant species, and can vary with growth environments and seasons (Bond-Lamberty et al., 2004a; Boone et al., 1998; Burton et al., 2012; Friedlingstein et al., 2020; Hanson et al., 2000; Jarvi & Burton, 2020; Markita et al., 2009, 2012; Pregitzer et al., 2000; Tang et al., 2019; Wang et al., 2010). The commonly measured total soil respiration (the soil-to-atmosphere flux at the soil surface, R_S) integrates both R_{root} and heterotrophic respiration (R_H); direct *in situ* measurements of R_{root} are rare (Ryan et al., 1997).

Quantifying the proportion of R_{root} to total R_S and the spatial patterns of this ratio has important implications for understanding the response of terrestrial ecosystems to climate change. R_{root} and R_H have different sources and sensitivities to biotic and abiotic drivers (Schindlbacher et al., 2009): the former is tightly coupled to current photosynthesis, whereas microbes oxidize soil organic carbon (SOC) that has been stored in the soil over potentially much longer periods of time (Trumbore, 2006). If photosynthesis and thus R_{root} increase with climate change, this constitutes an acceleration of the carbon cycle, but not necessarily a climate feedback. In contrast, an increase in heterotrophic activity raises the possibility of liberating long-stored SOC, producing a positive feedback (Bond-Lamberty et al., 2018).

Knowledge of R_{root}:R_S can also provide insight into terrestrial and atmosphere carbon exchange dynamics. For example, R_{root}:R_S is an important factor in calculating ecosystem- to global-scale net ecosystem production, the difference between net primary production (NPP) and R_H. At the global scale, NPP can usually be estimated from remote sensing, but belowground R_H is difficult to measure; instead, global R_S has been studied widely by upscaling from "bottom-up" site-scale measurements using statistical modelling approaches (Bond-Lamberty & Thomson, 2010a; Hashimoto et al., 2015; Jian, Steele, Day, et al., 2018; Jian, Steele, Thomas, et al., 2018; Lu et al., 2021; Raich & Potter, 1995; Raich et al., 2002; Warner et al., 2019). An understanding of the magnitude and global patterns of R_{root}:R_S thus bridges the gap between "top-down" NPP and "bottom-up" R_S estimates and is needed because of the difficulty of measuring R_{root} directly.

Measurement techniques to separate the commonly measured R_S (Jian, Bahn, et al., 2020) into R_{root} and R_H can be grouped into three broad categories: exclusion, component integration and isotopic (Hanson et al., 2000). The principle of root exclusion is that R_{root} can be estimated as the difference in CO_2 flux between *in situ* measurements with and without living roots (e.g., control sites compared with nearby bare soil, plots with roots removed, girdled plots, trenches). Exclusion is cheap to implement and widely used (Baah-Acheamfour et al., 2020; Kuzyakov, 2006; Li et al., 2016; Savage et al., 2018; Zhang, Cadotte, et al., 2019; Zhang, Li, et al., 2019; Zhao et al., 2016). The second method, component integration, involves measuring and then scaling specific rates of CO_2 flux from each component (typically, extracted roots, sieved soil and litter). Finally, isotopic approaches involve using radioactive elements (e.g., ^{14}C) to infer the origins of R_S *in situ*. Syntheses have not found any consistent differences in the results from these methods (Bond-Lamberty et al., 2004a; Subke et al., 2006). A fourth method of estimating R_{root} and/or R_H involves leveraging the commonly measured R_S and multi-site relationships from data syntheses. Bond-Lamberty et al. (2004a) analysed the variability of R_{root}:R_S and developed a global relationship between R_{root}:R_S and annual R_S. Subke et al. (2006) produced an independent analysis and developed a global relationship between R_H:R_S and annual R_S. These relationships, however, were based on only a few tens of measurements from forests. More recently, Zhao et al. (2021) developed a simple model to separate forest R_S based on root allometry. Beyond the spatial scale of the individual study site, attempts have been made to partition roots from R_H using modelling approaches and data syntheses (Lu et al., 2021; Tang et al., 2019, 2020). Most recently, site-scale measurements of R_S, including its components R_{root} and R_H, have been integrated into an updated global soil respiration database (SRDB) (Bond-Lamberty & Thomson, 2010b; Jian, Vargas, et al., 2021). The newest version, SRDB-V5, has 880 measurements of R_{root}:R_S, but no study has assessed global variations in R_{root}:R_S with many environmental factors using these data.

The overarching goal of the present study was to predict global R_{root}:R_S and understand the drivers of spatial variability in R_{root}:R_S. Specifically, our objectives were as follows: (1) to generate global estimates of R_{root}:R_S based on the new and improved SRDB-V5; (2) to determine the best statistical predictors (and their spatial pattern) of R_{root}:R_S at the global scale; (3) to produce a spatial R_{root}:R_S global product at 0.5° spatial resolution and examine its global pattern; and (4) to assess the older methods (Bond-Lamberty et al., 2004a; Subke et al., 2006) of predicting R_{root} directly from total R_S. To the best of our knowledge, this is the first analysis of the spatial patterns of R_{root}:R_S at a global scale.

2 | MATERIALS AND METHODS

2.1 | R_{root}:R_S training data

Field measurements of R_{root}:R_S and accompanying study characteristics (e.g., ecosystem types, partition method; Figure S1) were obtained from the newly updated global soil respiration database (SRDB-V5), a database of published studies about R_S. More details about SRDB-V5 are given by Jian, Vargas, et al. (2021) and https://github.com/bpbond/srdb. Here, we follow Bond-Lamberty et al. (2004a) in defining R_{root}:R_S as the annual R_{root} to annual R_S ratio; it is unitless, a proportion from zero to one.

SRDB-V5 is much larger than previous versions; R_{root}:R_S measurements increased from 634 in SRDB-V4 to 970 in SRDB-V5. Only R_{root}:R_S measurements meeting the following criteria were included in the present study: (1) annual (not only growing season) R_{root}:R_S was reported directly or could be calculated from reported data [e.g., as R_{root}:R_S = R_{root}/R_S or R_{root}:R_S = $(R_S - R_H)/R_S$]; (2) information on the latitude and longitude of measurement sites was available; (3) potentially problematic observations (those with a notation in the Quality_flag field of SRDB-V5) were excluded; and (4) reported or calculated R_{root}:R_S had to be between zero and one. With these criteria, we used 880 R_{root}:R_S observations, including 261 from agriculture, 140 from grasslands, 71 from savannas, 21 from shrublands, 256 from temperate and boreal forests, 70 from tropical forests, 2 from urban areas and 59 from wetlands (Figure 1; grouped according to "Ecosystem_type" and "leaf_habit" information in SRDB-V5). Although there were few observations from Australia, Russia, Africa and South America, this dataset covered all major ecosystem types (Friedl et al., 2002) and climate zones (Kottek et al., 2006) globally (Figure 1). All R_{root}:R_S data were measured between 1962 and 2015, with the amount of data increasing by year; at most sites, R_{root}:R_S was measured for <2 years; as the monitoring length of time increased, the amount of data decreased greatly (Figure S2).

It is important to note that there are many uncertainties in partitioning soil respiration into R_{root} and R_H that are impossible to quantify fully here. First, some R_{root} components (i.e., respiration from root-associated microorganisms and macrofauna in the rhizosphere) are difficult to separate in field experiments (Hanson et al., 2000). Second, it is harder and more expensive to separate R_S into R_{root} and R_H than simply measuring the overall total R_S, and therefore only a small proportion (*c.* 15%) of studies have measured R_H (or R_{root}) in field experiments (Jian, Vargas, et al., 2021). Finally, many different approaches are used for partitioning R_S, each with strengths and weaknesses and uncertain biases. We did not attempt to propagate these various uncertainties through analysis, but rather simply used R_{root}:R_S and R_S as reported by study authors and encoded in the SRDB.

2.2 | Environmental variables for predicting global R_{root}:R_S

We used a variety of global datasets of environmental variables available at a sufficient spatial scale to predict global R_{root}:R_S (Figure S1). Annual temperature, annual precipitation, mean annual temperature (MAT) and mean annual precipitation (MAP) between 1970 and 2013 were obtained from the WorldClim 2 data (Fick & Hijmans, 2017), and climate regions were obtained from the Köppen climate classification (Kottek et al., 2006). Atmospheric

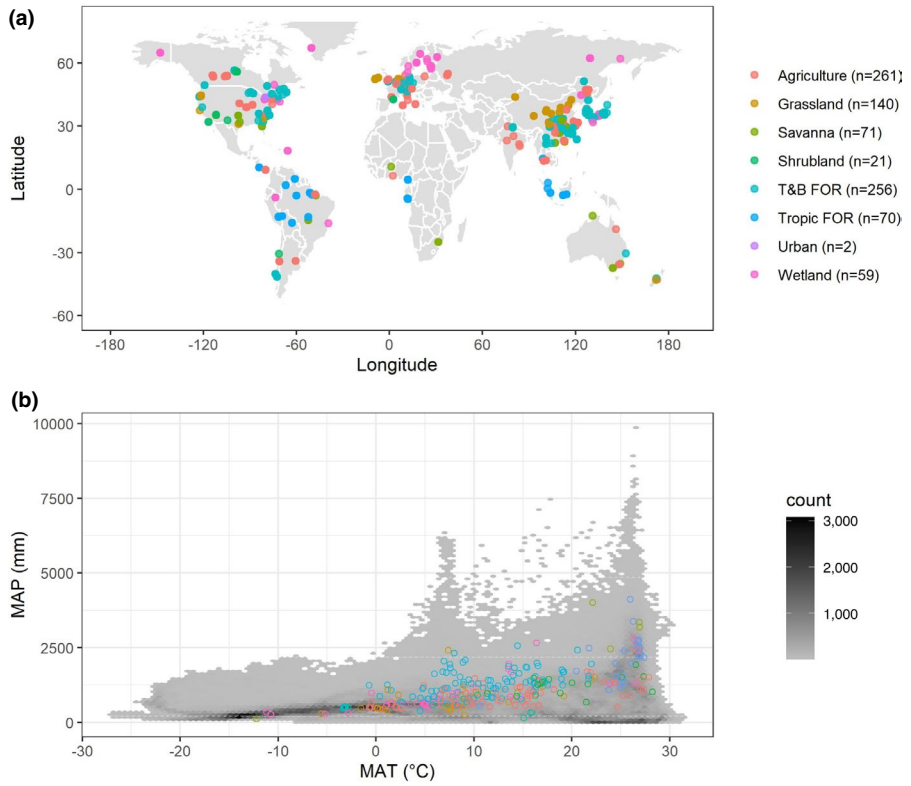

FIGURE 1 (a) Spatial distribution of the contribution of annual root respiration to soil respiration (R_{root}:R_S); sites are from the global soil respiration database (SRDB; n = 880). (b) Distribution of R_{root}:R_S sites (coloured markers) in entire global climate space (WorldClim v.2; Fick & Hijmans, 2017) of mean annual temperature (MAT) versus mean annual precipitation (MAP). Background colours indicate the number of half-degree grid cells with each MAT–MAP combination. Sites in different ecosystems were represented as different colours. T&B FOR = temperate and boreal forest; Tropic FOR = tropical forest

nitrogen (N) deposition with a resolution of 0.5° × 0.5° was downloaded from https://www.isimip.org/gettingstarted/details/24/, providing a time coverage between 1860 and 2017; we used the average between 1980 and 2017 because most R_{root}:R_S data were from this period (Figure S2). Soil variables, including SOC, soil bulk density and soil clay content (Clay, as a percentage), were from the SoilGrids 100 m dataset (Hengl et al., 2017). Arbuscular mycorrhiza (AM), Ectomycorrhiza (EcM), ericoid mycorrhiza (ErM) and non-mycorrhizal (NM) fractions were from a 0.167° × 0.167° global mycorrhizal plant distribution data product (Soudzilovskaia et al., 2019). Aboveground biomass (AGB) and belowground biomass (BGB) with a spatial resolution of 0.0028° × 0.0028° were from Spawn and Gibbs (2020). Given that R_S is a flux and is related not only to carbon stocks as biomass but also to ecosystem carbon flux, annual mean gross productivity data were also included. We aggregated monthly values of global gross primary productivity (GPP) from the 0.5° × 0.5° FLUXCOM data (Jung et al., 2020; Tramontana et al., 2016). Finally, global annual R_S data (1 km spatial resolution) were obtained from Warner et al. (2019). The latitude and longitude of R_{root}:R_S observations, in addition to leaf habit (i.e., evergreen, deciduous or mixed) of the ecosystem and partitioning method used, were retrieved directly from the SRDB-V5 (i.e., as reported in the original studies).

Vegetation types were obtained from the MODIS land cover type (Friedl et al., 2002), and MODIS enhanced vegetation index (EVI) data were used to represent vegetation greenness (Huete et al., 2002). Specifically, EVI, an optimized vegetation index, is a numerical combination of the near-infrared, red and blue bands (Huete et al., 2002). It is highly sensitive to vegetation canopy (e.g., leaf area index) and biomass variations and has been used widely to detect vegetation change and retrieve vegetation parameters, such as leaf area index and GPP (Boegh et al., 2002; Sjöström et al., 2011). All MODIS datasets were downloaded from the Google Earth Engine (GEE) platform (Huete et al., 2002). Specifically, we used 16-day MOD13A2 V6 terra vegetation indices with 1 km spatial resolution from 2000–2017 (Gorelick et al., 2017), and the MCD12Q1 V6 land cover type data in 2010 (Friedl et al., 2002) with 500 m spatial resolution. We only used the EVI data in the MOD13A2 with good quality indicated by quality assurance (QA) flags. We used the International Geosphere-Biosphere Programme (IGBP) classification layer in the MCD12Q1 to remove all pixels with the land cover types of snow/ice, water, barren and urban from our analysis.

The process of scaling site-level R_{root}:R_S measurements to global predictions requires ancillary global-scale raster data, as mentioned in Table 1. It is therefore necessary to evaluate the consistency between ancillary data from global rasters and that information measured and reported in the original papers. SRDB-V5 records MAT, MAP, soil bulk density and soil clay content if reported in the original papers; we compared these values with those from global rasters at the same geographical location and found they are fairly consistent (Figure S3). For other variables, however, we lack data from SRDB-V5 for such testing of consistency. Given that those rasters were peer reviewed and were evaluated with *in situ* measurements (for details, please see references mentioned above), we assume that their accuracy was similar to the data tested in the (Figure S3).

These global datasets are at different spatial resolutions (varying from 500 m to 0.5°; for details, see Table 1). The coarsest spatial resolution is 0.5° longitude, 0.5° latitude; therefore, we predicted global R_{root}:R_S at 0.5° × 0.5° spatial resolution. Variable datasets that were at higher spatial resolution than 0.5° × 0.5° (e.g., for the mycorrhizal dataset) were first resampled to 0.5° × 0.5° resolution using the area-weighted average method before use in the model. SRDB-V5 R_{root}:R_S observations are annual means; hence, our predicted R_{root}:R_S product was at an annual time-scale; temporal variables, such as temperature and precipitation, provided at sub-annual resolution, were aggregated to a 1970–2013 mean.

We used analysis of variation (ANOVA, using "aov" function in R, v.3.6.1) to investigate whether R_{root}:R_S is affected by the partitioning method (i.e., component, exclusion, isotope, other and physical separation), climate zones (from Kottek et al., 2006) and ecosystems (e.g., agriculture, forest, grassland, plantation, shrubland and wetland). If $p < .05$ for the ANOVA test, we used a Tukey's honest significant differences test (*TukeyHSD* in R) to test the differences between the means among different climate/vegetation/partitioning-method groups. For all other continuous environmental variables, we used linear least-squares regression to investigate whether R_{root}:R_S was significantly related to environmental variables.

2.3 | Random forest modelling

We predicted R_{root}:R_S at the global scale using random forest models from the spatial predictors described above, extracted to each field site location from the SRDB. Random forest is a regression tree-based bootstrapped nonparametric model, which allows large numbers of numerical and categorical input parameters (Breiman, 2001). Given that random forest might preferentially weight highly correlated variables, we performed a preliminary analysis on possible predictors. FLUXCOM-GPP and EVI are both vegetation-related variables that are highly correlated with each other (Figure S4). This correlation is likely to occur because FLUXCOM-GPP is a derived data product based, in part, on satellite greenness, from which EVI is calculated directly. Therefore, we decided to include the direct measurement of EVI while excluding FLUXCOM-GPP from the random forest model. Previous studies have found that R_{root}:R_S (or R_H:R_S) is closely correlated with annual R_S (Bond-Lamberty et al., 2004a; Subke et al., 2006). Based on this correlation, the annual R_S product from Warner et al. (2019) could conceivably be used to model R_{root}:R_S. However, our goal was to model R_{root}:R_S independent of annual R_S to allow for an unbiased, direct comparison with the R_{root}:R_S product from Warner et al. (2019); therefore, we excluded this variable from the random forest model.

When upscaling to global R_{root}:R_S, our focus is mean R_{root}:R_S across the whole study period (1962–2015) rather than global R_{root}:R_S for each year; therefore, annual temperature and annual precipitation were not used in the random forest model. From the

TABLE 1 Global variables used to predict the contribution of root respiration to soil respiration

Category	Variable	Time period (if applicable)	Spatial resolution	Unit	Sources
Climate	MAT	1970–2013	1 km	°C	Fick and Hijmans (2017)
	MAP	1970–2013	1 km	mm/year	
Nitrogen deposition	N deposition	1980–2017	0.5° × 0.5°	g N/m^2/year	Lamarque et al. (2013); https://www.isimip.org/gettingstarted/details/24/
Soil	Clay content	NA	1 km	%	Hengl et al. (2017); https://files.isric.org/soilgrids/former/2017-03-10/data/ (last accessed December 2020)
	Bulk density	NA	1 km	g/cm^3	
	SOC	NA	1 km	Mg C/ha	
Mycorrhizal	Arbuscular mycorrhiza (AM)	NA	0.167° × 0.167°	%	Soudzilovskaia et al. (2019); https://github.com/nasoudzilovskaia/Soudzilovskaia_NatureComm_MycoMaps/tree/master/Maps_Myco_veg_current
	Ectomycorrhiza (EcM)	NA	0.167° × 0.167°	%	
	Ericoid mycorrhiza (ErM)	NA	0.167° × 0.167°	%	
	Non-mycorrhizal (NM)	NA	0.167° × 0.167°	%	
Biomass	Aboveground biomass (AGB)	2010	0.0028° × 0.0028°	Mg C/ha	Spawn and Gibbs (2020); https://daac.ornl.gov/cgi-bin/dsviewer.pl?ds_id=1763
	Belowground biomass (BGB)	2010	0.0028° 0.0028°	Mg C/ha	
Enhanced vegetation index	EVI	2000–2017	1 km	Unitless	Huete et al. (2002); MODIS MOD13A2; GEE: https://earthengine.google.com/
Landcover	Landcover	2010	500 m	Unitless	Friedl et al. (2002); MODIS MCD12Q1; GEE: https://earthengine.google.com/

Abbreviation: NA: not applicable.

original list of candidate variables, we chose 14 environmental variables as input parameters to the random forest model: MAT, MAP, N deposition, soil clay percentage, soil bulk density, SOC, AM, EcM, ErM, NM, AGB, BGB and EVI (Table 1). Individual linear least-squares regressions ("lm" function in R) were fitted for each of the continuous predictors with R_{root}:R_S (Figure S5).

Random forest models were fitted using the 'randomForest' package (Liaw & Wiener, 2002) in R v.3.6.1 (R Core Team, 2019). We used the 'tuneRF' function in the 'randomForest' package to identify the appropriate number of variables for the random forest model. We then plotted the change of mean square error as the number of trees increased in the random forest model to identify the suitable number of trees, which we identified as 200. We set the number of variables tried in each tree split into four (Figure S6). The importance of individual input variables was tested as follows: (1) by quantifying the increase in model mean square error as each variable was removed ("tuneRF" function in the "randomForest" package); and (2) by visual examination of the partial dependence plots of each variable in the model ("partial" function in the "pdp" package).

For each tree in the random forest model, a subset of data was selected randomly by sampling with replacement from the original R_{root}:R_S samples, and the rest of data was used as a cross-validation dataset. This process was repeated 200 times (i.e., number of trees = 200). The resulting collection of trees (the random forest model) was then used to predict R_{root}:R_S from the global extent of the predictor rasters, with R_{root}:R_S pixel values calculated as the mean of the 200 random forest trees prediction at each pixel. Uncertainty was reported as the standard deviation (*SD*) of the 200 random forest trees prediction at each pixel, and the coefficient of variation (CV) was calculated by dividing the *SD* by the mean prediction at each pixel.

2.4 | Predicting root respiration through R_{root}:R_S

The relationships between annual R_S and R_{root}:R_S (Bond-Lamberty et al., 2004a) and between annual R_S and R_H:R_S (Subke et al., 2006) were used to derive global R_{root} and R_H (Hashimoto et al., 2015; Warner et al., 2019). However, in the present study we showed that no single factor could explain >2% of the variability of R_{root}:R_S. In order to evaluate bias in R_{root} predictions according to the relationship between R_{root}:R_S and annual R_S, we calculated global R_{root} by multiplying global R_{root}:R_S values developed in the present study by a global R_S product (Warner et al., 2019) (R_{root1}; Equation 1), and calculated values of global R_{root} were compared with the results from Warner et al. (2019) (R_{root2}; Equation 2). We mapped the difference between R_{root2} and R_{root1}, and the difference ratio (Equation 3), to investigate the potential bias and its spatial distribution if using the relationships between annual R_S and R_{root}:R_S to derive global R_{root}.

$$R_{root1} = R_S\,(\text{Warner et al., 2019}) \times R_{root}{:}\,R_S \quad (1)$$

$$R_{root2} = R_S\,(\text{Warner et al., 2019}) - R_H\,(\text{Warner et al., 2019}) \quad (2)$$

$$\text{Difference ratio} = \left(R_{root2} - R_{root1}\right) / \left[\frac{\left(R_{root2} + R_{root1}\right)}{2}\right] \quad (3)$$

3 | RESULTS

3.1 | Relationship between R_{root}:R_S and environmental factors

No single factor explained >2% of the variability in R_{root}:R_S. We analysed the relationship between R_{root}:R_S and annual R_S using 880 different pairs of measurements from the SRDB-V5. We found a significant relationship between R_{root}:R_S and annual R_S, with annual R_S explaining 2% of R_{root}:R_S variability ($p < .01$, $R^2 = .02$; black dots and line in Figure 2a). It is unlikely that extreme R_{root}:R_S values caused this change, because we obtained a similar curve when values of annual $R_S > 2500$ were excluded (grey line in Figure 2a). We investigated whether R_{root}:R_S was affected by partitioning method, climate and ecosystems, and we found that R_{root}:R_S measured by "component" was significantly different to that measured by "exclusion" and "other" methods ($p < .01$; Figure 2b). No difference was found among climate zones (Figure 2c). The R_{root}:R_S from "shrubland" was significantly different from the R_{root}:R_S of "wetland" ($p < .01$; Figure 2d).

The R_{root}:R_S exhibited a decreasing trend with time (Figure 3a); no significant relationship was found between R_{root}:R_S and annual temperature (Figure 3b), but we found a significant positive relationship between R_{root}:R_S and annual precipitation ($R^2 = .02$; Figure 3c). Soil bulk density and MAP had positive relationships (but not significant, $p > .05$) with R_{root}:R_S.

3.2 | Random forest modelling of R_{root}:R_S

Random forest modelling was used to predict R_{root}:R_S. The MAP, soil bulk density, EVI, BGB, SOC and MAT were the six most important variables according to change in mean squared error and node purity (Figure 4b,c). The model explained 51% of variability in R_{root}:R_S ($R^2 = .51$; Figure 5a). The MAP, EVI, NM and ErM were, in general, positively related to R_{root}:R_S, whereas SOC and AM were, in general, negatively related to R_{root}:R_S (see partial dependence plots in Figure S7). For all other variables, no consistent effect was found (Figure S7).

3.3 | Spatial patterns of global R_{root}:R_S

The MAP, soil bulk density and EVI were the three most important environmental factors driving R_{root}:R_S (Figure 4). From the random forest model, we predicted R_{root}:R_S, *SD* and CV of R_{root}:R_S across the globe at a spatial resolution of 0.5° (Figure 6; Figure S8). The area-weighted global mean R_{root}:R_S was .42 (i.e., 42% of global

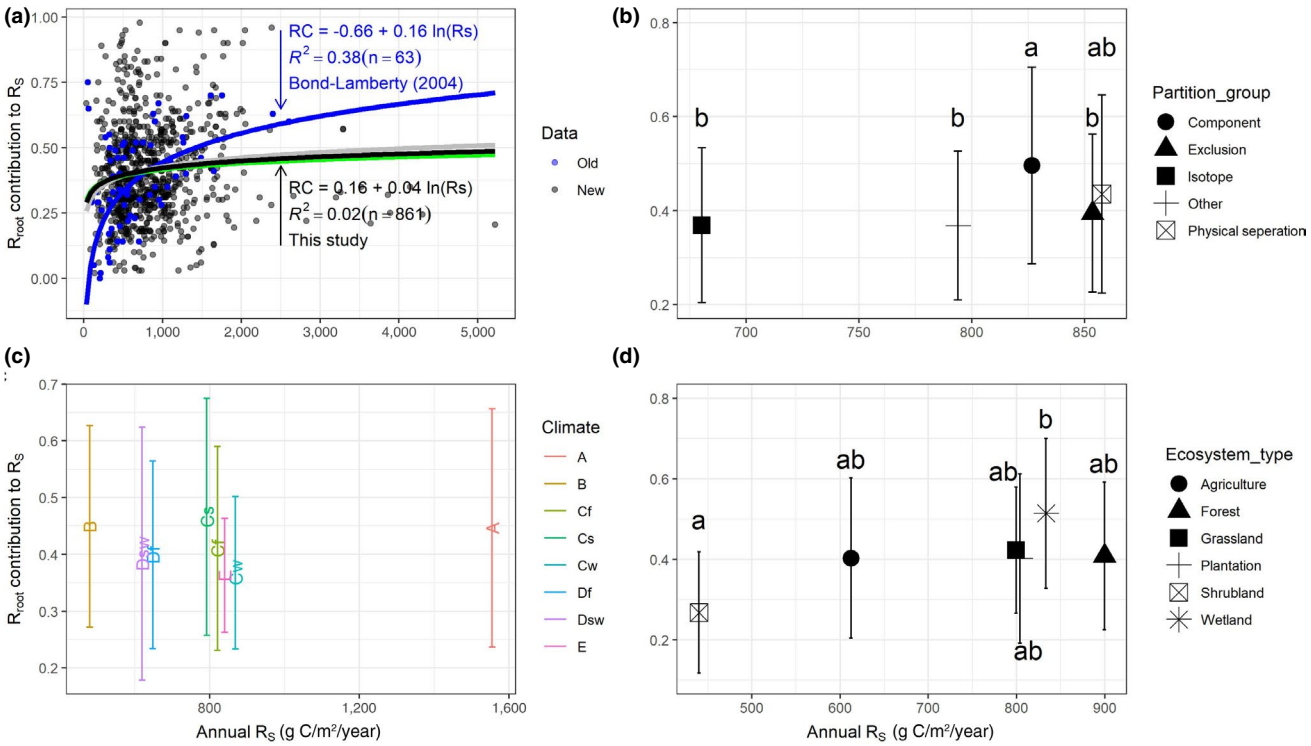

FIGURE 2 (a) The relationship between the contribution of root respiration to soil respiration (R_{root}:R_S) and annual soil respiration. The blue line shows the relationship developed by Bond-Lamberty et al. (2004a); the black line shows our relationship from all ecosystem types; the grey line excludes annual soil respiration >2500 g C/m^2/year; and the green line includes only measurements from forest. (b–d) Mean R_{root}:R_S values were calculated by different partitioning methods, climates and ecosystems, respectively, x-axis shows mean soil respiration for those categorical variables. The error bars are *SD*. Letters above the bars (in b,d) represent significant differences detected by Tukey's HSD pairwise comparison. A = tropic; B = arid; Cf = temperate humid; Cs = temperate summer dry; Cw = temperate winter dry; Df = boreal humid; Dsw = boreal summer dry or winter dry; E = arctic

R_S is generated by plant roots), with an *SD* of .18 and CV of 44%. Comparing the distribution of predicted R_{root}:R_S with the distribution of measured R_{root}:R_S from SRDB, predicted R_{root}:R_S was mainly distributed between .25 and .65, whereas the measured R_{root}:R_S from SRDB showed a much wider distribution (Figure 5b). This is a common feature of model outputs, because: (1) statistical models, by design, capture mean effects, not outliers; and (2) both statistical and process models are a function of the driving data used, which might miss extreme "hot spots" and "hot moments" in space and time. The predicted R_{root}:R_S showed a clear spatial pattern, with higher R_{root}:R_S values in the Arctic, Amazon regions in South America, South Africa and central Australia, but relatively low R_{root}:R_S in other regions (Figure 6). The *SD* of R_{root}:R_S prediction had a similar spatial pattern to R_{root}:R_S, and as a result, CV exhibited a relatively even distribution across the globe (Figure S8).

We calculated global R_{root} by multiplying global R_{root}:R_S values developed in the present study by a global R_S product (Warner et al., 2019). The calculated R_{root} showed a similar spatial pattern to the results of Warner et al. (2019; Figure 7a,b). Compared with global R_{root} calculated through R_{root}:R_S, Warner et al. (2019) overestimated R_{root} in the south-east USA, south-east China, Southeast Asia, South America and central Africa, but underestimated R_{root} for all other regions (Figure 7c).

4 | DISCUSSION

This is the first effort to produce a spatial product of global R_{root}:R_S, complementing previous R_H maps (Hashimoto et al., 2015; Lu et al., 2021; Tang et al., 2019, 2020; Warner et al., 2019). According to our random forest model, MAP was the most important variable globally for predicting R_{root}:R_S, followed by soil bulk density and EVI (Figure 4). The ratio of R_{root} to R_S results from a complex interaction of multiple variables, each of which varies spatially and independently. Precipitation has been found to affect vertical root distribution, plant and root growth (Kulmatiski & Beard, 2013; Zhang, Cadotte, et al., 2019; Zhang, Li, et al., 2019); therefore, its relationship with R_{root}:R_S is perhaps not surprising. This confirms the importance of soil water availability at different spatial and temporal scales in regulating elements of the global carbon cycle (Anderegg et al., 2015; Du et al., 2020; McDowell et al., 2020). Another soil property, soil bulk density, usually exhibits a negative relationship with SOC (Jian, Du, et al., 2020); it also reflects soil compaction level and is therefore linked to penetration and growth of plant roots (Ola et al., 2018). EVI, an optimized vegetation index, is highly sensitive to vegetation canopy (e.g., leaf area index) and biomass variations. Therefore, EVI has been used widely to detect change in vegetation and to retrieve vegetation parameters, such as leaf area index and GPP (Boegh et al., 2002; Sjöström et al., 2011). Our work emphasizes the value of global datasets

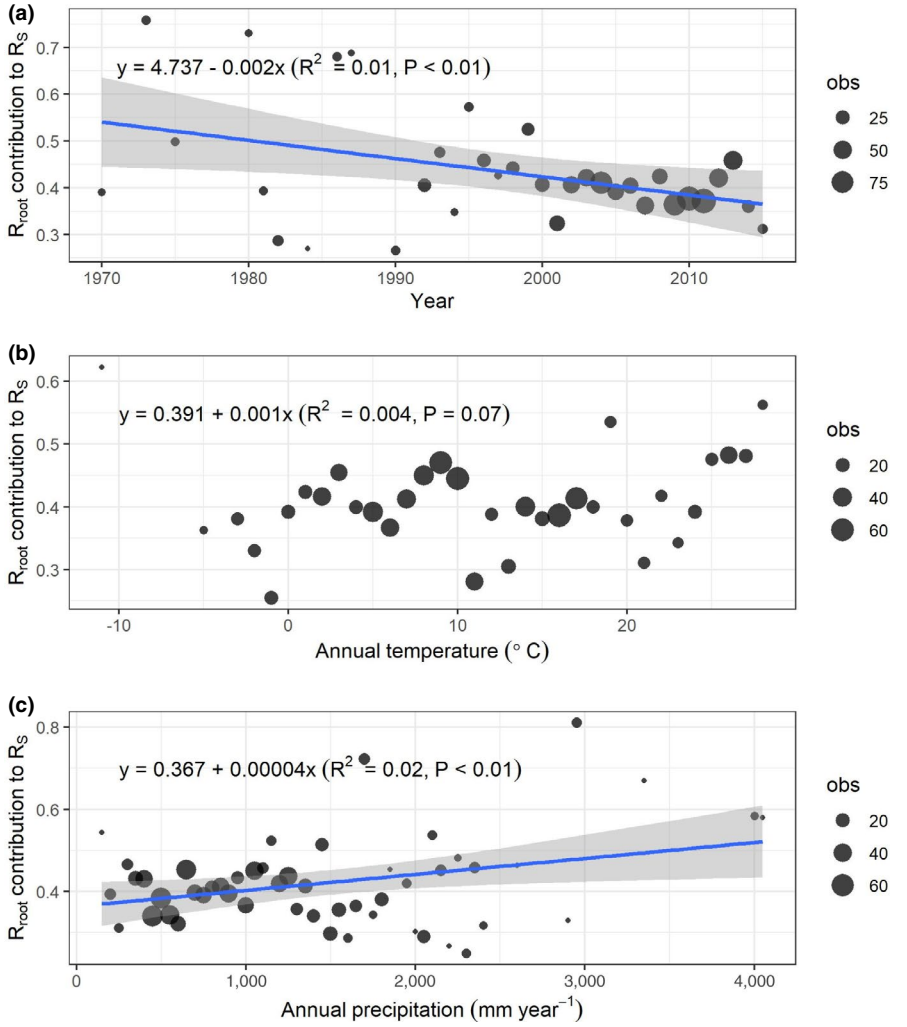

FIGURE 3 Relationship between the contribution of root respiration to soil respiration (R_{root}:R_S) and: (a) measurement year, (b) annual averaged temperature, or (c) annual precipitation. The linear regression is shown only if the significance level was $p < .05$; the 95% confidence interval is shown in grey. Note that the linear regression analysis was based on the raw data. For better visualization, we summarized R_{root}:R_S by year, annual temperature and annual precipitation (a–c, respectively), with the size of dot (i.e., "obs" in the key) representing the number of observations for a certain year, annual temperature or annual precipitation

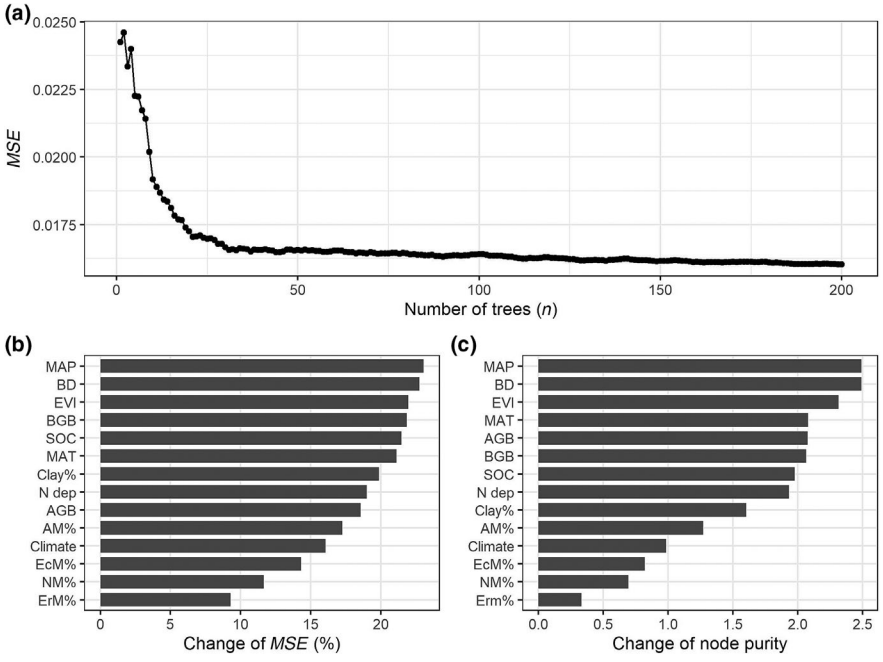

FIGURE 4 (a) Change of mean square error (*MSE*) values as the number of trees increases in the random forest model. (b) Change in *MSE* as each individual variable is removed from the model. (c) Change in node purity that results as each individual variable is removed from the model. Abbreviations: AGB, aboveground biomass; AM%, Arbuscular mycorrhiza (%); BD, soil bulk density; BGB, belowground biomass; Clay%, soil clay content (%); Climate, climate regions obtained from the Köppen climate classification (Kottek et al., 2006); EcM, Ectomycorrhiza (%), ErM, Ericoid mycorrhiza (%); EVI, enhanced vegetation index; MAP-mean annual precipitation; MAT, mean annual temperature; N dep, nitrogen deposition; NM, Non-mycorrhizal (%); SOC, soil organic carbon

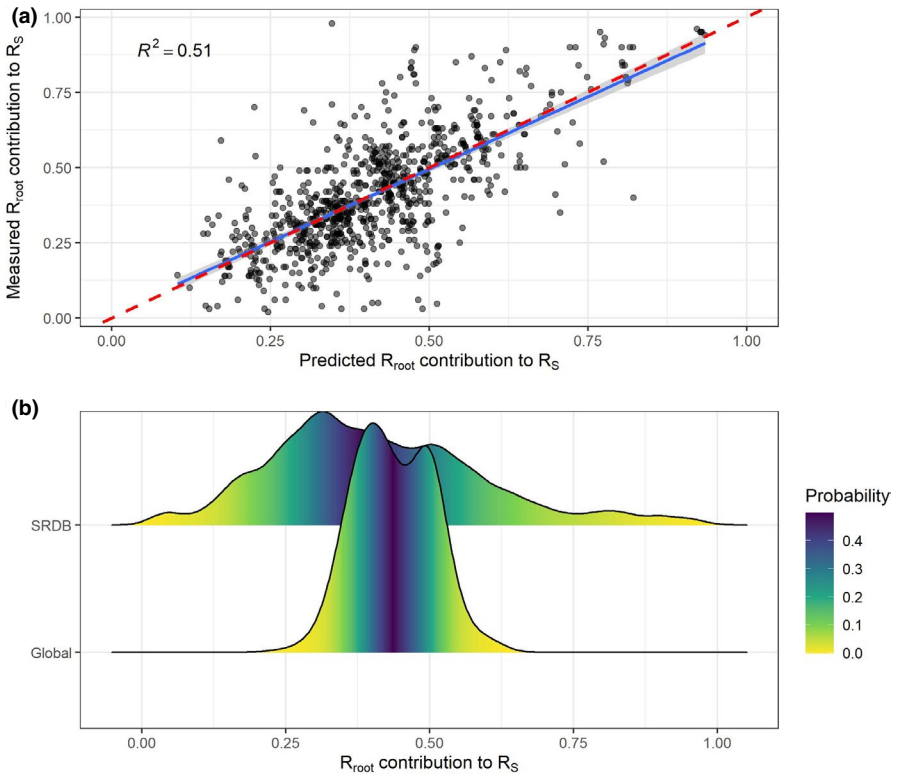

FIGURE 5 (a) Relationship between predicted contribution of root respiration to soil respiration (R_{root}:R_S) and measured R_{root}:R_S in the global soil respiration database (SRDB; $n = 880$). The red dashed line is the 1:1 trend, and the blue continuous line represents the linear regression between predicted and measured R_{root}:R_S. (b) Distributions of predicted R_{root}:R_S for the 880 SRDB sites and R_{root}:R_S prediction in the global

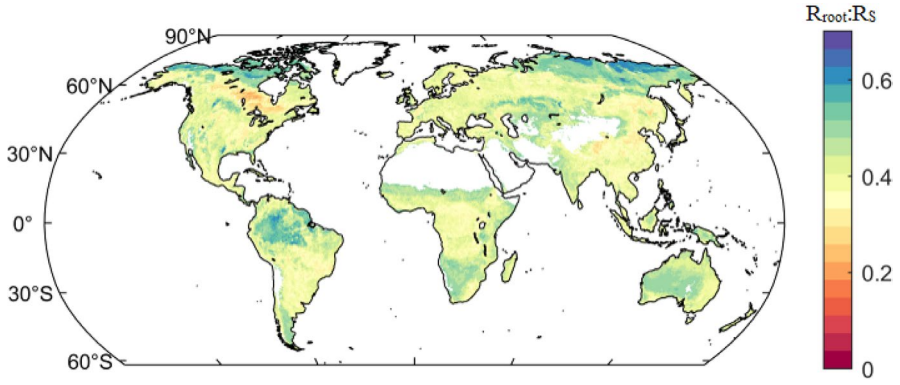

FIGURE 6 Global spatial distribution of the contribution of root respiration to soil respiration (R_{root}:R_S) predicted by the random forest model, with a spatial resolution of 0.5°. We used the International Geosphere–Biosphere Programme (IGBP) classification layer in MCD12Q1 to mask all pixels with the land cover types of snow/ice, water, barren and urban

on soil, climate and vegetation properties at spatial resolutions appropriate for the estimation of carbon fluxes across different geographical regions and ecosystem types. Further development and refinement of such spatial products will improve our ability to forecast changes in soil respiration over time and space accurately and precisely.

4.1 | Is robust prediction of R_{root}:R_S possible?

Root respiration is difficult to measure *in situ*; measuring R_H (and then computing R_{root} by subtraction) is somewhat easier but still laborious. For this reason, regression-based estimates (Bond-Lamberty et al., 2004a; Subke et al., 2006) are appealing. For example, Bond-Lamberty et al. (2004a) found, in forests, that R_{root}:R_S was significantly correlated with annual R_S and that annual R_S alone could explain 38% of R_{root}:R_S variability (and explained 81%–87% of R_A and R_H). Subke et al. (2006) presented a similar relationship explaining 30% of variability in R_H:R_S. These findings suggested that the magnitude of the single, easy-to-measure R_S flux could provide robust estimates of its heterotrophic and autotrophic sources, and these two papers have each been cited 500+ times in the last 15 years (searched by Google Scholar).

We reanalysed the relationship between R_{root}:R_S and annual R_S using an order of magnitude more data and found that annual R_S could explain only 2% of R_{root}:R_S variability (Figure 2a). This was true whether we included all ecosystem types or, as in the study by

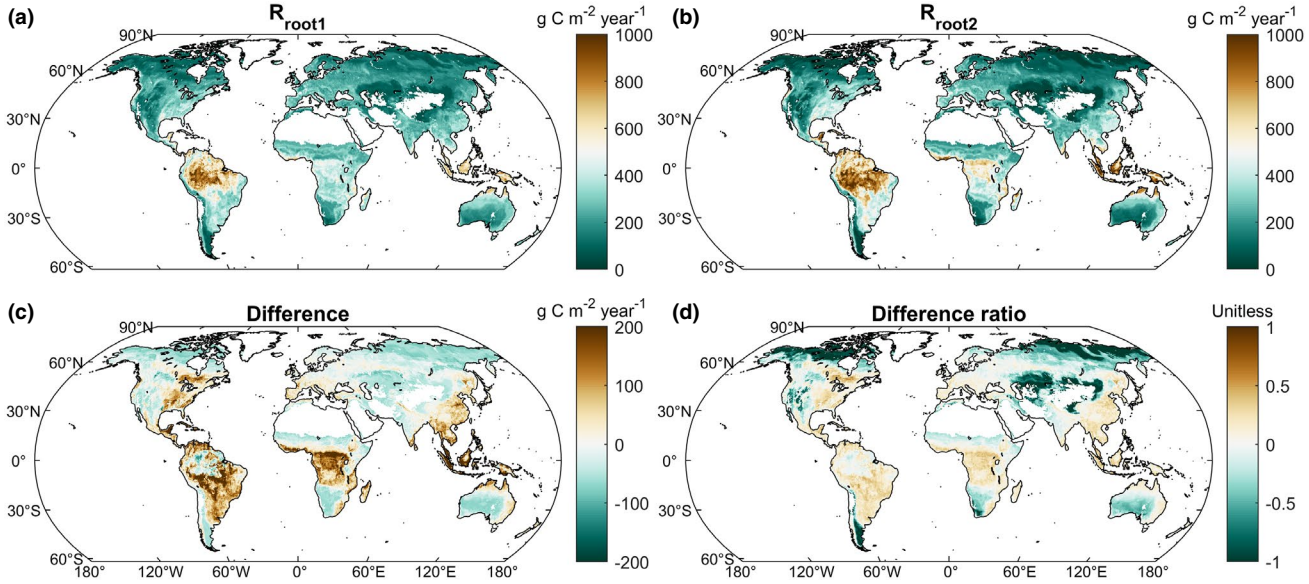

FIGURE 7 Comparison of two different methods for estimating root respiration (R_{root}). (a) R_{root} predicted by total soil respiration from Warner et al. (2019) × root contribution to soil respiration (R_{root}:R_S) from Figure 6 (R_{root1}; Equation 1). (b) R_{root} calculated as $R_{S,Warner}$ − $R_{H,Warner}$ (R_{root2}; Equation 2). (c) The difference in R_{root} calculated by the above two different methods (R_{root2} − R_{root1}). (d) The difference ratio calculated based on Equation (3) with a spatial resolution of 0.5°

Bond-Lamberty et al. (2004b), only forests (green line in Figure 2a). It appears, then, that the relatively strong predictive models presented by Bond-Lamberty et al. (2004b) and Subke et al. (2006) were primarily a function of the limited extant data at that time; the order of magnitude more data available today has far more unexplained variability (Hanson et al., 2000). The use of these equations could therefore contribute to substantial errors in estimation of carbon flux, similar to the use of simple plant carbon use efficiency (CUE, the ratio of net primary production gain to gross primary production during a period) models (DeLucia et al., 2007).

The higher variability in R_{root}:R_S now evident in the more comprehensive (compared with Bond-Lamberty et al., 2004a and Subke et al., 2006) SRDB-V5 database is likely to derive from many factors. Site- to ecosystem-scale R_{root} usually cannot be measured directly (Bond-Lamberty et al., 2004a; Hanson et al., 2000; Ryan et al., 1997; Subke et al., 2006); therefore, it is calculated as the difference between R_S and R_H and inherits error from both of those measured fluxes. In other words, if the measurement errors for R_S and R_H are σ_1 and σ_2, respectively, the error for R_{root} is roughly the sum of σ_1 and σ_2 (because $R_{root} = R_S - R_H$) in many conditions. In R_S modelling, soil temperature, precipitation and vegetation (e.g., EVI) are usually the most important variables to predict R_S (Hashimoto et al., 2015; Jian, Steele, Day, et al., 2018; Jian, Steele, Thomas, et al., 2018; Jian, Yuan, et al., 2021; Raich & Potter, 1995; Raich et al., 2002; Warner et al., 2019). Here, however, those variables explained only very limited variability of R_{root}:R_S, emphasizing the increased difficulty involved in predicting how root respiration contributes to total R_S at the soil surface.

What would produce large divergences in R_{root}:R_S from the relatively constant ecosystem means? A high value of R_{root}:R_S, i.e. high R_{root} relative to R_H, would imply low NPP (if R_H and NPP are assumed to be roughly in balance in non-disturbed systems) relative to GPP; in other words, low plant CUE (Curtis et al., 2005; DeLucia et al., 2007; Waring et al., 1998). As with plant CUE, time since disturbance is likely to affect R_{root}:R_S (Bond-Lamberty et al., 2004b; DeLucia et al., 2007), because both the initial disturbance and the ecological succession can strongly affect the carbon cycle (Amiro et al., 2010; Curtis et al., 2005).

Site-to-site R_{root}:R_S variability was high, but was not explained by differences in the ecosystems compared; the only significant difference in R_{root}:R_S was between shrubland and wetland (Figure 2d). This supports a previous meta-analysis, in which Subke et al. (2006) showed that the R_H:R_S ratio generally did not differ between four ecosystem types. This contrasts with plant CUE, which exhibits strong deviations between forest types (see Delucia et al., 2007: figure 2). However, R_{root}:R_S data were not distributed equally among the ecosystem types, potentially leading to bias (e.g., only 11 and 12 measurements for shrubland and wetland, respectively, hence the samples might not represent the overall mean of R_{root}:R_S; a similar issue exists for partitioning method and climate zones). We suggest that analysis of how plant CUE and R_{root}:R_S do, or do not, co-vary in geographical and ecological space would be a valuable future study.

4.2 | Implications of a global R_{root}:R_S product

The global R_{root}:R_S prediction map developed in the present study could be used to estimate global R_H and R_{root} in the future, and would be easy to update given new data. Several previous studies have predicted global R_H based on global R_S and a statistically

linear relationship between R_H and R_S, based on the work of Bond-Lamberty et al. (2004b), resulting in global R_H data products (Hashimoto et al., 2015; Warner et al., 2019). However, the results from the present study show that the relationship between R_S and R_{root}:R_S changes significantly with improved data representation across different ecosystems (Figure 2a). This indicates that predicting global R_H based on the relationship between annual R_S and R_{root}:R_S is fraught with uncertainty and, possibly, bias. The global R_{root}:R_S map produced here fills this gap, although we emphasize that its own uncertainties are large (see Figure 5). Alternatively, recent efforts have been made to predict R_H using random forest modelling (Lu et al., 2021; Tang et al., 2020). However, separating R_S into R_{root} and R_H in the field is difficult, and only *c*. 15% of studies have measured R_H (or R_{root}) in field experiments (Jian, Vargas, et al., 2021). Therefore, continuing to refine and improve this global R_{root}:R_S product will help to address a crucial need for future research on global carbon cycling.

Robust global R_{root}:R_S estimates could be a crucial link between "top-down" and "bottom-up" approaches in studies of the global terrestrial carbon cycle and provide a metric independent of plant CUE for evaluating and understanding ecosystem function (Figure 8). Terrestrial plants fix carbon from the atmosphere through photosynthesis, and roughly the same amount of carbon is returned to the atmosphere through respiration (i.e., R_{root}, R_H and aboveground autotrophic respiration). Although these two processes are fundamentally linked, they are usually studied separately: "top-down" approaches use models derived by satellite remote sensing technology to quantify GPP, whereas "bottom-up" approaches use direct measurements of R_S in different environments (Figure 8). However, only a fraction of R_S results from SOC decomposition, and there are also R_{root} and aboveground autotrophic respiration sources (Harmon et al., 2011). Therefore, although R_S measurements by themselves cannot determine GPP unambiguously, they can provide valuable constraints on its estimation (Barba et al., 2018; Phillips et al., 2017; Wang et al., 2017). Here, we show that R_H could be derived from "top-down" GPP (Equations 4 and 5; Figure 8) and "bottom-up" R_S measurements (Equations 6 and 7; Figure 8). The global R_{root}:R_S map and model presented here advance us toward linking "top-down" and "bottom-up" approaches (Equation 8; Figure 8).

4.3 | Limitation, uncertainties and future perspectives

Except for component methods, R_{root}:R_S showed no significant differences between different approaches; similar results were found in site-scale studies. R_{root}:R_S showed significant differences between component and exclusion methods (Figure 2b), and this difference is unlikely to be attributable to differences in R_S among categories, because we found no dependence of R_{root}:R_S on R_S. Results from

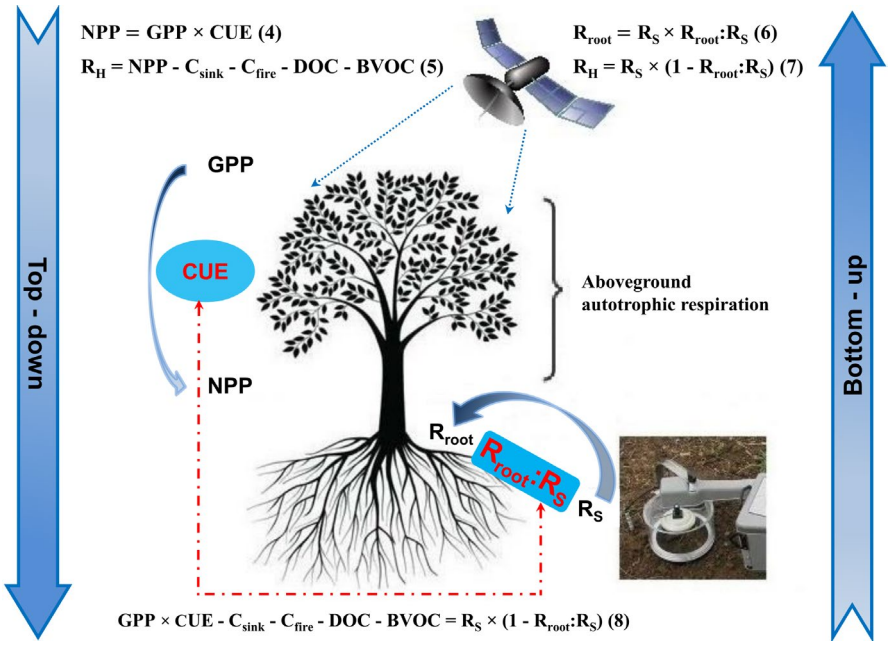

FIGURE 8 Conceptual diagram showing application of the contribution of root respiration to total soil respiration (R_{root}:R_S) in global terrestrial carbon cycling research. Left side: plant carbon use efficiency (CUE, defined as the ratio of net primary production gain to gross primary production during a period) is a crucial variable to estimate net primary production (NPP) from gross primary production (GPP × CUE; Equation 4), which is usually driven by data from remote sensing instruments; heterotrophic respiration (R_H) could be calculated by deducting carbon consumed by herbivores (C_{herb}), burned in fires (C_{fire}), exported as dissolved organic carbon (DOC) or returned to the atmosphere by biogenic volatile organic compound emissions (BVOC) of plants from NPP (Equation 5). Right side: R_{root}:R_S provides a crucial link between soil respiration (R_S), root respiration (R_{root}) and R_H (Equations 6 and 7). Therefore, R_{root}:R_S and plant CUE are crucial variables to link "top-down" and "bottom-up" carbon cycling research (Equation 8)

syntheses with unpaired data from different studies (sites), such as the present study, can be affected by differences in the environmental conditions among sites, and future field experiments could be designed at the same site, in the same conditions to test our findings. Most measurements of R_{root}:R_S used to build the random forest model in the present study were obtained by variants on the exclusion approach (n = 753 of 880, *c.* 86%); a similar proportion was reported in a previous meta-analysis by Subke et al. (2006). One disadvantage of the exclusion method is that dead roots can cause extra R_H, resulting in underestimation of R_{root}:R_S (Díaz-Pinés et al., 2010; Kuzyakov, 2006). In addition, compared with the control, soil moisture could be significantly different in the sites with roots excluded and could introduce bias (Savage et al., 2018). No systematic bias has been detected in relationship to the exclusion method, however; for example, Comeau et al. (2018) compared five partitioning approaches and found no overall strengths or weaknesses among them, and Bond-Lamberty et al. (2011) compared different trench approaches and found that they produced similar estimates of R_H.

Dividing R_S broadly into R_{root} and R_H means that differences between subcomponents within those groups are ignored. R_{root} can be separated further into maintenance respiration, growth of plant roots and rhizomicrobial respiration. However, in the field experiments, those components were usually not separated. Separating individual components of R_{root} is helpful to gain a better understanding of the mechanisms underlying total R_{root} and to improve the accuracy of partitioning in the future. Soudzilovskaia et al. (2019) presented a global dataset at high spatial resolution of arbuscular, ectomycorrhizal, ericoid mycorrhizal and non-mycorrhizal vegetation carbon storage; such datasets can, potentially, be used to explore this question further in the future.

With respect to prediction errors, the uneven spatial distribution of R_{root}:R_S measurements might cause bias in the global R_{root}:R_S map. Most R_{root}:R_S measurements used in the present study to build the random forest model are from the middle latitudes of the Northern Hemisphere (Figure 1). The most economically developed countries are in northern middle-latitude regions, which means that more funds and experts are available to support on-site R_{root}:R_S measurement there. Measuring R_{root}:R_S in the Southern Hemisphere is more urgent in the future. For the Arctic, however, it is particularly hard to measure R_S during long, cold winters, and most experiments in the Arctic operate only during the growing season (Jian, Bahn, et al., 2020). Using data with a finer time-scale, such as daily or monthly R_{root}:R_S, could resolve this issue, in part, because sites measured only in growing season could be used in this scenario (Jian, Steele, Thomas, et al., 2018). Regardless, we emphasize that users of the global R_{root}:R_S map produced in the present study should be aware of and consider the prediction errors included with the predicted R_{root}:R_S values.

Temporal variability of R_{root}:R_S under ongoing global changes of temperature, precipitation and carbohydrates from photosynthesis should be explored in the future. In the present study, we focused on the global R_{root}:R_S spatial pattern and its controlling environmental factors. However, whether R_{root}:R_S responds to global changes of temperature, precipitation and carbohydrates from photosynthesis and how it might affect future climate change is a crucial question. Previous studies found that global R_S showed a clear temporal trend to increase under global climate change (Bond-Lamberty et al., 2018; Bond-Lamberty & Thomson, 2010a; Tang et al., 2019, 2020). We found that R_{root}:R_S showed a significant trend to decrease with time (Figure 3a), implying that the increased R_S comes from R_H, which raises the possibility of liberating long-stored SOC, producing a positive feedback (Bond-Lamberty et al., 2018). Jarvi and Burton (2020) found that R_{root} showed acclimation in experimental soil warming conditions, indicating that R_{root}:R_S might respond to global warming under climate change, which is consistent with our findings that R_{root}:R_S exhibited a significant negative trend with measuring time (Figure 3a). Furthermore, a positive relationship with annual precipitation (Figure 3c) suggests that change in global precipitation under global warming might play an important role in carbon–climate feedbacks.

4.4 | Conclusion

In recent decades, the growing abundance and far-reaching locations of research studies that measure soil respiration partitions have made it possible to predict R_{root}:R_S statistically on a global scale and analyse its spatial pattern. This study is the first attempt to leverage >800 observations in the soil respiration database to predict global R_{root}:R_S and analyse its spatial pattern. Based on R_{root}:R_S measurements from an updated global soil respiration database, we showed that global variability in R_{root}:R_S cannot be predicted by any one of the global environmental variables that were tested. We produced a global map of R_{root}:R_S using random forest modelling, combining 14 different spatial environmental datasets as predictors. The area-weighted overall mean of predicted R_{root}:R_S in the globe is .42 (SD ± .18). By using data-driven modelling of an experimentally derived variable, our global R_{root}:R_S product lies somewhere between "top-down" remote sensing-based estimates of primary production and "bottom-up"-based respiration measurements. This product has helped to highlight: (1) high variability of R_{root}:R_S, with no single factor explaining its variability; (2) current knowledge gaps in linking plant CUE to soil respiration processes; and (3) persistent geographical biases in terrestrial carbon cycle field studies.

ACKNOWLEDGMENTS

This research was supported by the second Tibetan Plateau Scientific Expedition and Research Program (STEP; number 2019QZKK0603) and the U.S. Department of Energy, Office of Science, Biological and Environmental Research as part of the Terrestrial Ecosystem Sciences Program. The Pacific Northwest National Laboratory is operated for Department of Energy by Battelle Memorial Institute under contract DE-AC05-76RL01830.

CONFLICT OF INTEREST

There are no conflicts of interest.

AUTHOR CONTRIBUTIONS

Ben Bond-Lamberty and Jinshi Jian conceived this study and designed the primary analysis. Max Frissell performed the primary analysis. Dalei Hao prepared remote sensing datasets. Xiaolu Tang performed the dominant variables analysis. Erin Berryman provided insightful comments in all phases. Jinshi Jian and Ben Bond-Lamberty wrote the manuscript in close collaboration with all authors. All authors provided feedback in all phases.

DATA AVAILABILITY STATEMENT

All data and code to reproduce the results in this study can be found at: https://github.com/jinshijian/SoilRespirationPartitioning. To summarize: users need first to download some datasets through the given website and the GitHub repository release attachment (Table S1), then to run the "*drake.R*" file to prepare all the data, followed by "*SRPartitioning.R*", which should be able to reproduce all the results. For descriptions of all the datasets, please see Table 1 and the (Table S1).

ORCID

Jinshi Jian https://orcid.org/0000-0002-5272-5367
Xiaolu Tang https://orcid.org/0000-0001-5079-7650

REFERENCES

Amiro, B. D., Barr, A. G., Barr, J. G., Black, T. A., Bracho, R., Brown, M., Chen, J., Clark, K. L., Davis, K. J., Desai, A. R., Dore, S., Engel, V., Fuentes, J. D., Goldstein, A. H., Goulden, M. L., Kolb, T. E., Lavigne, M. B., Law, B. E., Margolis, H. A., … Xiao, J. (2010). Ecosystem carbon dioxide fluxes after disturbance in forests of North America. *Journal of Geophysical Research*, *115*(G00K02), 1–13. https://doi.org/10.1029/2010jg001390

Anderegg, W. R. L., Hicke, J. A., Fisher, R. A., Allen, C. D., Aukema, J., Bentz, B., Hood, S., Lichstein, J. W., Macalady, A. K., McDowell, N., Pan, Y., Raffa, K., Sala, A., Shaw, J. D., Stephenson, N. L., Tague, C., & Zeppel, M. (2015). Tree mortality from drought, insects, and their interactions in a changing climate. *New Phytologist*, *208*(3), 674–683. https://doi.org/10.1111/nph.13477

Baah-Acheamfour, M., Carlyle, C. N., Bork, E. W., & Chang, S. X. (2020). Forest and perennial herbland cover reduce microbial respiration but increase root respiration in agroforestry systems. *Agricultural and Forest Meteorology*, *280*, 107790. https://doi.org/10.1016/j.agrformet.2019.107790

Barba, J., Cueva, A., Bahn, M., Barron-Gafford, G. A., Bond-Lamberty, B., Hanson, P. J., Jaimes, A., Kulmala, L., Pumpanen, J., Scott, R. L., Wohlfahrt, G., & Vargas, R. (2018). Comparing ecosystem and soil respiration: Review and key challenges of tower-based and soil measurements. *Agricultural and Forest Meteorology*, *249*, 434–443. https://doi.org/10.1016/j.agrformet.2017.10.028

Boegh, E., Soegaard, H., Broge, N., Hasager, C. B., Jensen, N. O., Schelde, K., & Thomsen, A. (2002). Airborne multispectral data for quantifying leaf area index, nitrogen concentration, and photosynthetic efficiency in agriculture. *Remote Sensing of Environment*, *81*(2–3), 179–193. https://doi.org/10.1016/S0034-4257(01)00342-X

Bond-Lamberty, B., Bailey, V. L., Chen, M., Gough, C. M., & Vargas, R. (2018). Globally rising soil heterotrophic respiration over recent decades. *Nature*, *560*(7716), 80–83. https://doi.org/10.1038/s41586-018-0358-x

Bond-Lamberty, B., Bronson, D., Bladyka, E., & Gower, S. T. (2011). A comparison of trenched plot techniques for partitioning soil respiration. *Soil Biology and Biochemistry*, *43*(10), 2108–2114. https://doi.org/10.1016/j.soilbio.2011.06.011

Bond-Lamberty, B., & Thomson, A. (2010a). Temperature-associated increases in the global soil respiration record. *Nature*, *464*(7288), 579–582. https://doi.org/10.1038/nature08930

Bond-Lamberty, B., & Thomson, A. (2010b). A global database of soil respiration data. *Biogeosciences*, *7*(6), 1915–1926. https://doi.org/10.5194/bg-7-1915-2010

Bond-Lamberty, B., Wang, C., & Gower, S. T. (2004a). A global relationship between the heterotrophic and autotrophic components of soil respiration? *Global Change Biology*, *10*(10), 1756–1766. https://doi.org/10.1111/j.1365-2486.2004.00816.x

Bond-Lamberty, B., Wang, C., & Gower, S. T. (2004b). Contribution of root respiration to soil surface CO_2 flux in a boreal black spruce chronosequence. *Tree Physiology*, *24*(12), 1387–1395. https://doi.org/10.1093/treephys/24.12.1387

Boone, R. D., Nadelhoffer, K. J., Canary, J. D., & Kaye, J. P. (1998). Roots exert a strong influence on the temperature sensitivity of soil respiration. *Nature*, *396*(6711), 570–572. https://doi.org/10.1038/25119

Breiman, L. (2001). Random forests. *Machine Learning*, *45*(1), 5–32. https://doi.org/10.1023/A:1010933404324

Burton, A. J., Jarvey, J. C., Jarvi, M. P., Zak, D. R., & Pregitzer, K. S. (2012). Chronic N deposition alters root respiration-tissue N relationship in northern hardwood forests. *Global Change Biology*, *18*(1), 258–266. https://doi.org/10.1111/j.1365-2486.2011.02527.x

Comeau, L.-P., Lai, D. Y. F., Cui, J. J., & Farmer, J. (2018). Separation of soil respiration: A site-specific comparison of partition methods. *SOIL*, *4*(2), 141–152. https://doi.org/10.5194/soil-4-141-2018

Curtis, P. S., Vogel, C. S., Gough, C. M., Schmid, H. P., Su, H.-B., & Bovard, B. D. (2005). Respiratory carbon losses and the carbon-use efficiency of a northern hardwood forest, 1999–2003. *The New Phytologist*, *167*(2), 437–455. https://doi.org/10.1111/j.1469-8137.2005.01438.x

DeLucia, E. H., Drake, J. E., Thomas, R. B., & Gonzalez-Meler, M. (2007). Forest carbon use efficiency: Is respiration a constant fraction of gross primary production? *Global Change Biology*, *13*(6), 1157–1167. https://doi.org/10.1111/j.1365-2486.2007.01365.x

Díaz-Pinés, E., Schindlbacher, A., Pfeffer, M., Jandl, R., Zechmeister-Boltenstern, S., & Rubio, A. (2010). Root trenching: A useful tool to estimate autotrophic soil respiration? A case study in an Austrian mountain forest. *European Journal of Forest Research*, *129*(1), 101–109. https://doi.org/10.1007/s10342-008-0250-6

Du, Y., Wang, Y. P., Su, F., Jiang, J., Wang, C., Yu, M., & Yan, J. (2020). The response of soil respiration to precipitation change is asymmetric and differs between grasslands and forests. *Global Change Biology*, *26*(10), 6015–6024. https://doi.org/10.1111/gcb.15270

Fick, S. E., & Hijmans, R. J. (2017). WorldClim 2: New 1-km spatial resolution climate surfaces for global land areas. *International Journal of Climatology*, *37*(12), 4302–4315. https://rmets.onlinelibrary.wiley.com/doi/abs/ https://doi.org/10.1002/joc.5086

Friedl, M. A., McIver, D. K., Hodges, J. C. F., Zhang, X. Y., Muchoney, D., Strahler, A. H., Woodcock, C. E., Gopal, S., Schneider, A., Cooper, A., Baccini, A., Gao, F., & Schaaf, C. (2002). Global land cover mapping from MODIS: Algorithms and early results. *Remote Sensing of Environment*, *83*(1), 287–302. https://doi.org/10.1016/S0034-4257(02)00078-0

Friedlingstein, P., O'Sullivan, M., Jones, M. W., Andrew, R. M., Hauck, J., Olsen, A., Peters, G. P., Peters, W., Pongratz, J., Sitch, S., Le Quéré, C., Canadell, J. G., Ciais, P., Jackson, R. B., Alin, S., Aragão, L. E. O. C., Arneth, A., Arora, V., Bates, N. R., … Zaehle, S. (2020). Global carbon budget 2020. *Earth System Science Data*, *12*(4), 3269–3340. https://doi.org/10.5194/essd-12-3269-2020

Gorelick, N., Hancher, M., Dixon, M., Ilyushchenko, S., Thau, D., & Moore, R. (2017). Google Earth Engine: Planetary-scale geospatial analysis for everyone. *Remote Sensing of Environment*, *202*, 18–27. https://doi.org/10.1016/j.rse.2017.06.031

Hanson, P. J., Edwards, N. T., Garten, C. T., & Andrews, J. A. (2000). Separating root and soil microbial contributions to soil respiration:

A review of methods and observations. *Biogeochemistry*, *48*(1), 115–146. https://idp.springer.com/authorize/casa?redirect_uri=https://link.springer.com/article/https://doi.org/10.1023/A:1006244819642&casa_token=bcG3mPS4r9sAAAAA:wexrf2X6p4ab_MRicorie5B1fUAYats_Hv82vHSNsdEX6x0YVxnE15znOGJxXHEuKnmQXXhoFy8p1d56Dg

Harmon, M. E., Bond-Lamberty, B., Tang, J., & Vargas, R. (2011). Heterotrophic respiration in disturbed forests: A review with examples from North America. *Journal of Geophysical Research*, *116*(G00K04), 1–17. https://doi.org/10.1029/2010jg001495

Hashimoto, S., Carvalhais, N., Ito, A., Migliavacca, M., Nishina, K., & Reichstein, M. (2015). Global spatiotemporal distribution of soil respiration modeled using a global database. *Biogeosciences*, *12*(13), 4121–4132. https://pure.mpg.de/pubman/faces/ViewItemOverviewPage.jsp?itemId=item_2161024

Hengl, T., Mendes de Jesus, J., Heuvelink, G. B. M., Ruiperez Gonzalez, M., Kilibarda, M., Blagotić, A., Shangguan, W., Wright, M. N., Geng, X., Bauer-Marschallinger, B., Guevara, M. A., Vargas, R., MacMillan, R. A., Batjes, N. H., Leenaars, J. G. B., Ribeiro, E., Wheeler, I., Mantel, S., & Kempen, B. (2017). SoilGrids250m: Global gridded soil information based on machine learning. *PLoS One*, *12*(2), e0169748. https://doi.org/10.1371/journal.pone.0169748

Huete, A., Didan, K., Miura, T., Rodriguez, E. P., Gao, X., & Ferreira, L. G. (2002). Overview of the radiometric and biophysical performance of the MODIS vegetation indices. *Remote Sensing of Environment*, *83*(1), 195–213. https://doi.org/10.1016/S0034-4257(02)00096-2

Jarvi, M. P., & Burton, A. J. (2020). Root respiration and biomass responses to experimental soil warming vary with root diameter and soil depth. *Plant and Soil*, *451*(1–2), 435–446. https://doi.org/10.1007/s11104-020-04540-1

Jian, J., Bahn, M., Wang, C., Bailey, V., & Bond-Lamberty, B. (2020). Prediction of annual soil respiration from its flux at mean annual temperature. *Agricultural and Forest Meteorology*, *287*, 107961. https://doi.org/10.1016/j.agrformet.2020.107961

Jian, J., Du, X., Reiter, M. S., & Stewart, R. D. (2020). A meta-analysis of global cropland soil carbon changes due to cover cropping. *Soil Biology and Biochemistry*, *143*, 107735. https://doi.org/10.1016/j.soilbio.2020.107735

Jian, J., Steele, M. K., Day, S. D., & Thomas, R. Q. (2018). Future global soil respiration rates will swell despite regional decreases in temperature sensitivity caused by rising temperature. *Earth's Future*, *6*(11), 1539–1554. https://agupubs.onlinelibrary.wiley.com/doi/abs/ https://doi.org/10.1029/2018EF000937

Jian, J., Steele, M. K., Thomas, R. Q., Day, S. D., & Hodges, S. C. (2018). Constraining estimates of global soil respiration by quantifying sources of variability. *Global Change Biology*, *24*(9), 4143–4159. https://doi.org/10.1111/gcb.14301

Jian, J., Vargas, R., Anderson-Teixeira, K., Stell, E., Herrmann, V., Horn, M., Kholod, N., Manzon, J., Marchesi, R., Paredes, D., & Bond-Lamberty, B. (2021). A restructured and updated global soil respiration database (SRDB-V5). *Earth System Science Data Discussions*, *13*(2), 255–267. https://doi.org/10.5194/essd-13-255-2021

Jian, J., Yuan, X., Steele, M. K., Du, C., & Ogunmayowa, O. (2021). Soil respiration spatial and temporal variability in China between 1961 and 2014. *European Journal of Soil Science*, *72*(2), 739–755. https://doi.org/10.1111/ejss.13061

Jung, M., Schwalm, C., Migliavacca, M., Walther, S., Camps-Valls, G., Koirala, S., Anthoni, P., Besnard, S., Bodesheim, P., Carvalhais, N., Chevallier, F., Gans, F., Groll, D. S., Haverd, V., Köhler, P., Ichii, K., Jain, A. K., Liu, J., Lombardozzi, D., … Reichstein, M. (2020). Scaling carbon fluxes from eddy covariance sites to globe: synthesis and evaluation of the FLUXCOM approach. *Biogeosciences*, *17*(5), 1343–1365. https://doi.org/10.5194/bg-17-1343-2020

Kottek, M., Grieser, J., Beck, C., Rudolf, B., & Rubel, F. (2006). World Map of the Köppen-Geiger climate classification updated. *Meteorologische Zeitschrift*, *15*(3), 259–263. https://doi.org/10.1127/0941-2948/2006/0130

Kulmatiski, A., & Beard, K. H. (2013). Woody plant encroachment facilitated by increased precipitation intensity. *Nature Climate Change*, *3*(9), 833–837. https://doi.org/10.1038/NCLIMATE1904

Kuzyakov, Y. (2006). Sources of CO_2 efflux from soil and review of partitioning methods. *Soil Biology & Biochemistry*, *38*(3), 425–448. https://doi.org/10.1016/j.soilbio.2005.08.020

Lamarque, J.-F., Dentener, F., McConnell, J., Ro, C.-U., Shaw, M., Vet, R., Bergmann, D., Cameron-Smith, P., Dalsoren, S., Doherty, R., Faluvegi, G., Ghan, S. J., Josse, B., Lee, Y. H., MacKenzie, I. A., Plummer, D., Shindell, D. T., Skeie, R. B., Stevenson, D. S., … Nolan, M. (2013). Multi-model mean nitrogen and sulfur deposition from the Atmospheric Chemistry and Climate Model Intercomparison Project (ACCMIP): evaluation of historical and projected future changes. *Atmospheric Chemistry and Physics*, *13*(6), 7997–8018. https://doi.org/10.5194/acp-13-7997-2013

Li, Y., Hou, C., Song, C., & Guo, Y. (2016). Seasonal changes in the contribution of root respiration to total soil respiration in a freshwater marsh in Sanjiang Plain, Northeast China. *Environmental Earth Sciences*, *75*(10), 848. https://doi.org/10.1007/s12665-016-5592-7

Liaw, A., & Wiener, M. (2002). Classification and regression by randomForest. *R News*, *2*(3), 18–22. https://www.researchgate.net/profile/Andy_Liaw/publication/228451484_Classification_and_Regression_by_RandomForest/links/53fb24cc0cf20a45497047ab/Classification-and-Regression-by-RandomForest.pdf

Lu, H., Li, S., Ma, M., Bastrikov, V., Chen, X., Ciais, P., Dai, Y., Ito, A., Ju, W., Lienert, S., Lombardozzi, D., Lu, X., Maignan, F., Nakhavali, M., Quine, T., Schindlbacher, A., Wang, J., Wang, Y., Wårlind, D., … Yuan, W. (2021). Comparing machine learning-derived global estimates of soil respiration and its components with those from terrestrial ecosystem models. *Environmental Research Letters*, *16*(5), 054048. https://doi.org/10.1088/1748-9326/abf526

Makita, N., Hirano, Y., Dannoura, M., Kominami, Y., Mizoguchi, T., Ishii, H., & Kanazawa, Y. (2009). Fine root morphological traits determine variation in root respiration of *Quercus serrata*. *Tree Physiology*, *29*(4), 579–585. https://doi.org/10.1093/treephys/tpn050

Makita, N., Kosugi, Y., Dannoura, M., Takanashi, S., Niiyama, K., Kassim, A. R., & Nik, A. R. (2012). Patterns of root respiration rates and morphological traits in 13 tree species in a tropical forest. *Tree Physiology*, *32*(3), 303–312. https://doi.org/10.1093/treephys/tps008

McDowell, N. G., Allen, C. D., Anderson-Teixeira, K., Aukema, B. H., Bond-Lamberty, B., Chini, L., Clark, J. S., Dietze, M., Grossiord, C., Hanbury-Brown, A., Hurtt, G. C., Jackson, R. B., Johnson, D. J., Kueppers, L., Lichstein, J. W., Ogle, K., Poulter, B., Pugh, T. A. M., Seidl, R., … Xu, C. (2020). Pervasive shifts in forest dynamics in a changing world. *Science*, *368*(6494), eaaz9463. https://doi.org/10.1126/science.aaz9463

Ola, A., Schmidt, S., & Lovelock, C. E. (2018). The effect of heterogeneous soil bulk density on root growth of field-grown mangrove species. *Plant and Soil*, *432*(1), 91–105. https://doi.org/10.1007/s11104-018-3784-5

Phillips, C. L., Bond-Lamberty, B., Desai, A. R., Lavoie, M., Risk, D., Tang, J., Todd-Brown, K., & Vargas, R. (2017). The value of soil respiration measurements for interpreting and modeling terrestrial carbon cycling. *Plant and Soil*, *413*(1), 1–25. https://doi.org/10.1007/s11104-016-3084-x

Pregitzer, K. S., King, J. S., Burton, A. J., & Brown, S. E. (2000). Responses of tree fine roots to temperature. *New Phytologist*, *147*(1), 105–115. https://nph.onlinelibrary.wiley.com/doi/abs/ https://doi.org/10.1046/j.1469-8137.2000.00689.x

R Core Team. (2019). *R: A language and environment for statistical computing, version 3.6.1*. R Foundation for Statistical Computing. https://www.R-project.org/

Raich, J. W., & Potter, C. S. (1995). Global patterns of carbon dioxide emissions from soils. *Global Biogeochemical Cycles*, *9*(1), 23–36. https://doi.org/10.1029/94GB02723

Raich, J. W., Potter, C. S., & Bhagawati, D. (2002). Interannual variability in global soil respiration, 1980–94. *Global Change Biology*, *8*(8), 800–812. https://doi.org/10.1046/j.1365-2486.2002.00511.x

Ryan, M. G., Lavigne, M. B., & Gower, S. T. (1997). Annual carbon cost of autotrophic respiration in boreal forest ecosystems in relation to species and climate. *Journal of Geophysical Research*, *102*(D24), 28871–28883. https://doi.org/10.1029/97jd01236

Savage, K. E., Davidson, E. A., Abramoff, R. Z., Finzi, A. C., & Giasson, M.-A. (2018). Partitioning soil respiration: Quantifying the artifacts of the trenching method. *Biogeochemistry*, *140*(1), 53–63. https://doi.org/10.1007/s10533-018-0472-8

Schindlbacher, A., Zechmeister-Boltenstern, S., & Jandl, R. (2009). Carbon losses due to soil warming: Do autotrophic and heterotrophic soil respiration respond equally? *Global Change Biology*, *15*(4), 901–913. https://doi.org/10.1111/j.1365-2486.2008.01757.x

Sjöström, M., Ardö, J., Arneth, A., Boulain, N., Cappelaere, B., Eklundh, L., De Grandcourt, A., Kutsch, W. L., Merbold, L., Nouvellon, Y., & Scholes, R. J. (2011). Exploring the potential of MODIS EVI for modeling gross primary production across African ecosystems. *Remote Sensing of Environment*, *115*(4), 1081–1089. https://doi.org/10.1016/j.rse.2010.12.013

Soudzilovskaia, N. A., van Bodegom, P. M., Terrer, C., Zelfde, M. V., McCallum, I., McCormack, M. L., Fisher, J. B., Brundrett, M. C., de Sá, N. C., & Tedersoo, L. (2019). Global mycorrhizal plant distribution linked to terrestrial carbon stocks. *Nature Communications*, *10*(1), 5077. https://doi.org/10.1038/s41467-019-13019-2

Spawn, S. A., & Gibbs, H. K. (2020). Global aboveground and belowground biomass carbon density maps for the year 2010. *ORNL DAAC*. https://daac.ornl.gov/cgi-bin/download.pl?ds_id=1763&source=schema_org_metadata

Subke, J.-A., Inglima, I., & Cotrufo, M. F. (2006). Trends and methodological impacts in soil CO_2 efflux partitioning: A metaanalytical review. *Global Change Biology*, *12*(6), 921–943. https://doi.org/10.1111/j.1365-2486.2006.01117.x

Tang, X., Fan, S., Du, M., Zhang, W., Gao, S., Liu, S., Chen, G., Yu, Z., Yao, Y., & Yang, W. (2020). Spatial and temporal pattern of global soil heterotrophic respiration in terrestrial ecosystems. *Earth System Science Data*, *12*(2), 1037–1051. https://doi.org/10.5194/essd-12-1037-2020

Tang, X., Fan, S., Zhang, W., Gao, S., Chen, G., & Shi, L. (2019). Global variability in belowground autotrophic respiration in terrestrial ecosystems, *Earth System Science Data*, *11*(4), 1839–1852. https://doi.org/10.5194/essd-11-1839-2019

Tramontana, G., Jung, M., Schwalm, C. R., Ichii, K., Camps-Valls, G., Ráduly, B., Reichstein, M., Arain, M. A., Cescatti, A., Kiely, G., Merbold, L., Serrano-Ortiz, P., Sickert, S., Wolf, S., & Papale, D. (2016). Predicting carbon dioxide and energy fluxes across global FLUXNET sites with regression algorithms. *Biogeosciences*, *13*(14), 4291–4313. https://doi.org/10.5194/bg-13-4291-2016

Trumbore, S. (2006). Carbon respired by terrestrial ecosystems – recent progress and challenges. *Global Change Biology*, *12*(2), 141–153. https://doi.org/10.1111/j.1365-2486.2006.01067.x

Wang, W., Chen, W., & Wang, S. (2010). Forest soil respiration and its heterotrophic and autotrophic components: Global patterns and responses to temperature and precipitation. *Soil Biology and Biochemistry*, *42*(8), 1236–1244. https://doi.org/10.1016/j.soilbio.2010.04.013

Wang, X., Wang, C., & Bond-Lamberty, B. (2017). Quantifying and reducing the differences in forest CO_2-fluxes estimated by eddy covariance, biometric and chamber methods: A global synthesis. *Agricultural and Forest Meteorology*, *247*, 93–103. https://doi.org/10.1016/j.agrformet.2017.07.023

Waring, R. H., Landsberg, J. J., & Williams, M. (1998). Net primary production of forests: A constant fraction of gross primary production? *Tree Physiology*, *18*(2), 129–134. https://doi.org/10.1093/treephys/18.2.129

Warner, D. L., Bond-Lamberty, B., Jian, J., Stell, E., & Vargas, R. (2019). Spatial predictions and associated uncertainty of annual soil respiration at the global scale. *Global Biogeochemical Cycles*, *33*(12), 1733–1745. https://doi.org/10.1029/2019GB006264

Zhang, B., Cadotte, M. W., Chen, S., Tan, X., You, C., Ren, T., Chen, M., Wang, S., Li, W., Chu, C., Jiang, L., Bai, Y., Huang, J., & Han, X. (2019). Plants alter their vertical root distribution rather than biomass allocation in response to changing precipitation. *Ecology*, *100*(11), e02828. https://doi.org/10.1002/ecy.2828

Zhang, B., Li, W., Chen, S., Tan, X., Wang, S., Chen, M., Ren, T., Xia, J., Huang, J., & Han, X. (2019). Changing precipitation exerts greater influence on soil heterotrophic than autotrophic respiration in a semiarid steppe. *Agricultural and Forest Meteorology*, *271*, 413–421. https://doi.org/10.1016/j.agrformet.2019.03.019

Zhao, C., Miao, Y., Yu, C., Zhu, L., Wang, F., Jiang, L., Hui, D., & Wan, S. (2016). Soil microbial community composition and respiration along an experimental precipitation gradient in a semiarid steppe. *Scientific Reports*, *6*, 24317. https://doi.org/10.1038/srep24317

Zhao, X., Liang, N., Zeng, J., & Mohti, A. (2021). A simple model for partitioning forest soil respiration based on root allometry. *Soil Biology & Biochemistry*, *152*, 108067. https://doi.org/10.1016/j.soilbio.2020.108067

SUPPORTING INFORMATION

Additional supporting information may be found in the online version of the article at the publisher's website.

How to cite this article: Jian, J., Frissell M., Hao D., Tang X., Berryman E., & Bond-Lamberty B. (2022). The global contribution of roots to total soil respiration. *Global Ecology and Biogeography*, 31, 685–699. https://doi.org/10.1111/geb.13454